

# EVOLUTION OF THE HADRONIC SYSTEM CREATED IN RELATIVISTIC HEAVY-ION COLLISIONS

*D.V. Anchishkin*<sup>1\*</sup>, *A.O. Muskeyev*<sup>2</sup>, *V.Yu. Vovchenko*<sup>2</sup>, and *S.N. Yezhov*<sup>2</sup>

<sup>1</sup>*Bogolyubov Institute for Theoretical Physics, Kiev, Ukraine*

<sup>2</sup>*Taras Shevchenko Kiev National University, Kiev, Ukraine*

(Received November 2, 2011)

Evolution of the hadronic system in heavy-ion collisions is studied with the reaction density. The three-dimensional reaction zones and their projections for different types of hadronic reactions are calculated for AGS and SPS energies within the microscopic transport model UrQMD. On the basis of performed calculations of reaction frequencies, the characteristic points of the time dependence of fireball evolution are obtained. The hypersurfaces which are the reaction zone boundaries are related to kinetic and chemical freeze-outs. The reaction density fireball representation is compared to other possible representations.

PACS: 25.75.-q, 25.75.Ag, 24.10.Lx

## 1. INTRODUCTION

A strongly interacting hadronic system is formed in heavy-ion collisions. A fireball is identified with a space-time region, in which the hadronic reactions occur. Hence, reaction zones must reflect the space-time characteristics of a fireball, and its study gives information about evolution of a fireball.

In the study of nucleus-nucleus collisions one can distinguish different stages of fireball evolution. Depending on a model describing the system, we can distinguish the regions of the formation of a fireball, its isotropization and thermalization, the creation of particles, the regions of a chemical freeze-out and a kinetic one, etc. As parameters for the determination of the stages of evolution of a system and the freeze-out process, one can take the particle density  $n(t, \mathbf{r})$  [1], energy density  $\epsilon(t, \mathbf{r})$  [2], temperature  $T(t, \mathbf{r})$  [3, 4], mean free path, rate of collisions of particles, etc. Depending on the chosen parameter one can get different fireball representations. In the present work, we use the hadron reaction density (number of reactions in a unit volume per unit time) in a given four-dimensional region of the space-time as a parameter of the spatial evolution of the interacting system. Such a quantitative estimate allows one to define the reaction zone, whose study gives a possibility to establish the space-time structure of a fireball from the viewpoint of the interaction intensity at every point of the space-time. The regions of a fireball can be distinguished by the interaction intensity which can be characterized by the number of collisions in a unit volume of the space-time. We use this quantity to determine the boundaries between different reaction zones.

Another important question which can be clari-

fied by the study of the zone of reactions is how the space-time boundary of a fireball is related to the processes of kinetic and chemical freeze-outs. Since the kinetic freeze-out is the process of establishment of a final distribution of hadrons in the momentum space, the sharp kinetic freeze-out hypersurface is an imaginary hypersurface, outside of which there are no collisions between radiated hadrons. In that sense the space-time boundary of a reaction zone and the sharp kinetic freeze-out hypersurface can be put in correspondence.

## 2. REACTION ZONES

The number of reactions in the given space-time region can be determined, for instance, with the use of the distribution function  $f(x, p)$ . The probability of a collision of two particles with momenta  $p_1$  and  $p_2$  corresponding to the distribution functions  $f_1$  and  $f_2$ , respectively, in the approximation of two-particle reactions  $2 \rightarrow 2$  is determined at a space-time point  $x$  as

$$P(x, \mathbf{p}_1, \mathbf{p}_2) = \int_3 \int_4 W_{12 \rightarrow 34} f(x, \mathbf{p}_1) f(x, \mathbf{p}_2). \quad (1)$$

The quantity  $W_{12 \rightarrow 34}$  is the transition rate which involves the reaction cross section and the conservation laws,  $\int_i \equiv \int \frac{d^3 p_i}{E_{p_i}}$ ,  $E_{p_i} = \sqrt{m^2 + \mathbf{p}_i^2}$ .

By integrating over the momenta of particles, we obtain the rate or the 4-density of reactions at the point  $x$ :

$$\Gamma(x) = \int_1 \int_2 \int_3 \int_4 W_{12 \rightarrow 34} f(x, \mathbf{p}_1) f(x, \mathbf{p}_2). \quad (2)$$

Then, the number of reactions in the given space-time

\*Corresponding author E-mail address: anch@bitp.kiev.ua

region  $\Omega$  is

$$N_{\text{coll}}(\Omega) = \int_{\Omega} d^4x \Gamma(x). \quad (3)$$

It is seen that the number of reactions in the given space-time region depends on the 4-density of reactions  $\Gamma(x)$  which can be determined in a certain model approximation, e.g., like that in [5, 6]. In particular,  $\Gamma(x)$  can be determined with the use of transport models.

The reaction zone is defined as the space-time region where a certain fraction of all reactions of certain type took place. This space-time region is chosen in a way that it was the most intense with respect to the reaction rate, that is, it has the smallest possible volume. Reaction zone can be associated with the flame from a candle (Fig. 1). It is the region which is the most intense with respect to exothermic reactions and is basically a reaction zone. The reaction zones for the given reaction type can be calculated by using the 4-density of reactions (2). Detailed description of the procedure one can find in Ref. [7]. Reaction zone can be calculated for different types of reactions. Reactions can be classified by type and number of hadrons taking part in these reactions (see the table).

*Reaction classification by number of participants*

1	$1 \rightarrow 2' + m, m \geq 0$	decay
2	$2 \rightarrow 1'$	fusion
3	$2 \rightarrow 2$	elastic scattering
4	$2 \rightarrow 2' + m, m \geq 0$	inelastic reaction

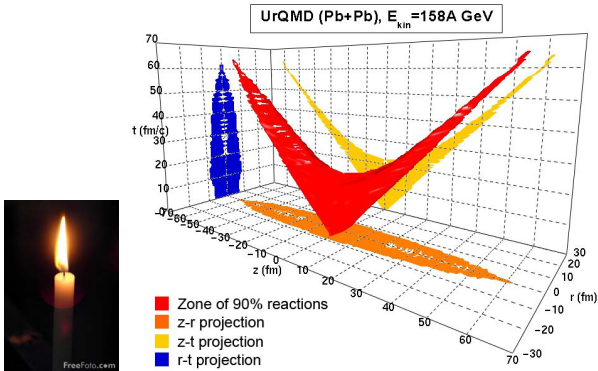


**Fig. 1.** Left: a candle, with a flame corresponding to the region where reactions take place. Right: the three-dimensional reaction zone, which determines the space-time region where 90% of all hadronic reactions for SPS conditions ( $E_{\text{kin}} = 158A \text{ GeV}$ ) take place

To carry out calculations, we use the transport model UrQMD v2.3 [8, 9] which allows one to calculate the four-density of hadronic reactions at every point of the space-time region and to select reactions of a given type and for the given species of particles. We take the number of reactions  $N_{\text{coll}}[\Omega(t, \mathbf{r})]$  in a pixel  $\Omega(t, \mathbf{r})$  as a result of the averaging over 1000 events. In the calculations, we took a four-cube of reactions  $C_R$  with the size of edges  $L_i = 200 \text{ fm}$ ,

where  $i = t, x, y, z$ . In Fig. 1 we show calculation results for conditions at the CERN Super Proton Synchrotron (SPS), Pb+Pb at 158A GeV in the case of central collisions. The figure depicts space-time region where 90% of all hadronic reactions take place. For this calculations we use coordinates  $(t, r, z)$  where  $r = \pm\sqrt{x^2 + y^2}$ . Also, different projections of the three-dimensional reaction zone are shown at coordinate planes:  $z$ - $t$  (yellow),  $r$ - $t$  (blue) and  $z$ - $r$  (orange). We note that the reaction density (2) does not depend on the azimuthal angle  $\varphi$  because of the symmetry of central collisions. Then, we deal with the reaction zone which is related to inelastic ( $2 \rightarrow 2' + m, m \geq 0$ ) hadronic reactions. By applying the same procedure the three-dimensional reaction zones for inelastic processes is obtained. Fig. 2 depicts calculation results for conditions at the BNL Alternating Gradient Synchrotron (AGS), Au+Au, and at the CERN Super Proton Synchrotron (SPS), Pb+Pb. By comparing the calculation results for all reactions (Fig. 1) and for inelastic reactions (Fig. 2) one can see that the reaction zone which contains 90% of all reactions roughly coincides with the reaction zone containing 99% of all inelastic reactions. We name this zone as region of hot fireball.

Henceforth, we will deal with the projection of the reaction zone on the  $z$ - $t$  plane. To design this projection we sum first all collisions along the transverse direction at the fixed coordinates  $(t, z)$ . Then, the reaction density in  $z$ - $t$  plane takes following form:

$$\tilde{\Gamma}(t, z) = \int dx dy \Gamma(t, x, y, z). \quad (4)$$

Then, the number of reactions in the given pixel  $\tilde{\Omega}(t, z)$  on  $z$ - $t$  plane is

$$\tilde{N}_{\text{coll}}[\tilde{\Omega}(t, z)] = \int_{\tilde{\Omega}(t, z)} dt dz \tilde{\Gamma}(t, z). \quad (5)$$

Then, the reaction zone projection can be constructed with the use of above-mentioned algorithm from Ref. [7].

In Fig. 3 we show the results of calculations for conditions at the BNL-AGS, Au+Au, and at the CERN-SPS, Pb+Pb, in the case of central collisions. In accordance with our algorithm, the four-volume which contains 99% of all hadronic inelastic reactions,  $2 \rightarrow 2' + m, m \geq 0$  is determined [depicted as the medium-grey (red) area]. As previously mentioned, this zone is named as a region of hot fireball. We determine also a four-volume that contains 99% of all possible hadronic reactions which include, of course, the previous zone. We name the region of 99% of all hadronic reactions excluding the zone of the hot fireball as a cold fireball [dark-grey (blue) area]. The additional region [light-grey (cyan) area] is a fireball halo and it contains additional 0.9% of all hadronic reactions. This zone is formed mostly by decays of resonances. That is, the three space-time regions (hot, cold, halo) cover 99.9% of the total number  $N_{\text{tot}}$  of all hadronic reactions.

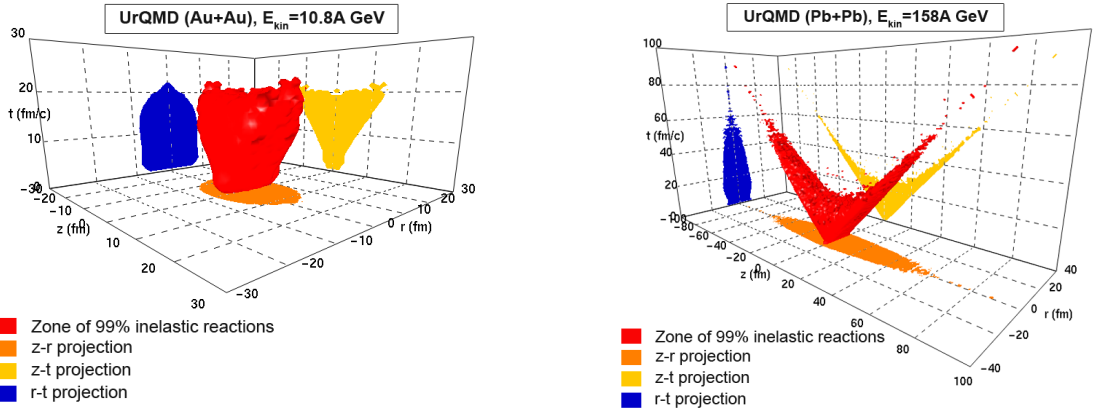


**Fig. 2.** The three-dimensional reaction zones, which determine the space-time region where 99% of all inelastic hadronic reactions for AGS conditions ( $E_{\text{kin}} = 10.8A \text{ GeV}$ ) and SPS conditions ( $E_{\text{kin}} = 158A \text{ GeV}$ ) take place

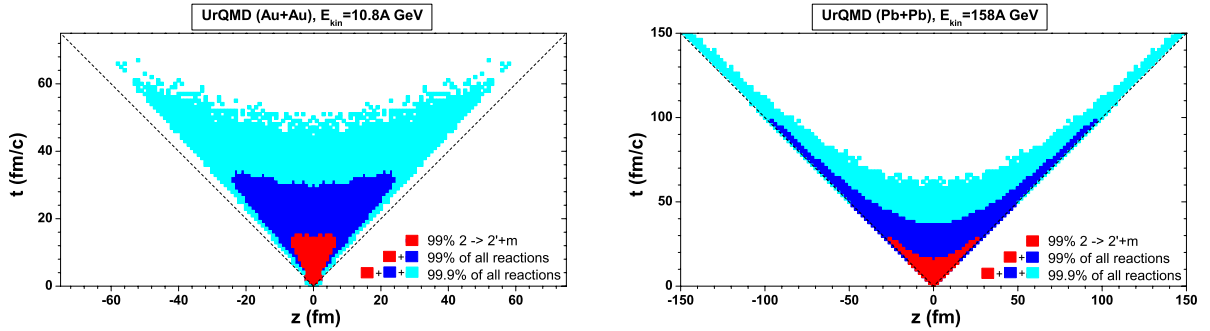


**Fig. 3.** Projection of the reaction zone on the  $z$ - $t$  plane under the AGS ( $Au+Au$  at  $10.8A \text{ GeV}$ ) and SPS ( $Pb+Pb$  at  $158A \text{ GeV}$ ) conditions. The medium-grey (red) region contains 99% of all inelastic reactions,  $2 \rightarrow 2' + m$ ,  $m \geq 0$ . The medium-grey (red) and the dark-grey (blue) regions together contain 99% of all hadronic reactions. The light-grey (cyan) region contains 0.9% of all hadron reactions only

It is seen that the interacting system has a comparatively long lifetime: A hot fireball decays completely only in the time intervals of the order of 15... 20 fm/c for AGS and 20... 35 fm/c for SPS. A cold fireball lives for 30... 33 fm/c for AGS and 80... 100 fm/c for SPS.

The zones of hot and cold fireballs together contain 99% of all reactions by definition. We can compare this reaction zone with the zone which is wrapped by freeze-out hypersurface. Note, following the “classical” definition of the sharp kinetic freeze-out hypersurface it is some boundary that separates the interacting system from the space-time domain where particles do not interact and almost all particles are evaporated (frozen out) from the thin space-time layer determined by this hypersurface. Then, it seems evident that the sharp kinetic freeze-out hypersurface should be inside reaction zone and not outside of it. And, in addition, the sharp chemical freeze-out hypersurface should be inside the hypersurface which separates the region of a hot fireball which contains 99% of all inelastic reactions.

### 3. REACTION FREQUENCY

Hadronic reactions can be classified by type and number of participants in these reactions (see the table) and the contributions of different types of reactions

into the system evolution can be explored. For this purpose we analyze the time dependence of reaction frequency for different types,  $i$ , of reactions:

$$\nu_i(t) = \int_{C_R} dx dy dz \Gamma_i(t, \mathbf{r}). \quad (6)$$

The results of evaluations of the time dependence of the reaction frequency (6) for AGS and SPS energies are depicted in Fig. 4. The thick solid line indicates all reaction rates in the fireball, the thin solid line indicates only the elastic scattering of hadrons ( $2 \rightarrow 2$ ), the dash-dotted line shows all inelastic reactions ( $2 \rightarrow 2' + m$ , where  $m \geq 0$ ), the dotted line stands for fusion reactions ( $2 \rightarrow 1'$ ), and the dashed line distinguishes decays ( $1 \rightarrow 2' + m$ ,  $m \geq 0$ ).

The main feature of the reaction frequency (thick solid lines in Fig. 4) is its increase up to  $t \simeq 5... 8 \text{ fm/c}$  for AGS energies and  $t \simeq 1... 2 \text{ fm/c}$  for SPS energies where it has its first maximum  $t_{m1}$ . This can be explained by the increase of the number of nucleons as participants of the reactions, when one nucleus penetrates into another one. The maximum overlap of two nuclei happens when their centers coincide. This time can be estimated as

$$t_c = \frac{R_0}{\gamma v}. \quad (7)$$

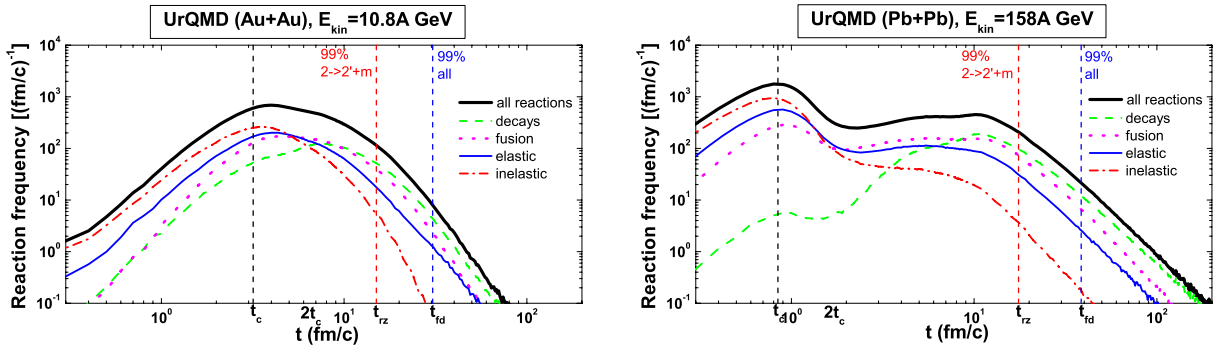


**Fig. 4.** Hadron reaction frequency for AGS (Au+Au at 10.8A GeV) and SPS (Pb+Pb at 158A GeV) conditions. Different curves correspond to different types of reactions

Here  $R_0$  is the nucleus radius,  $v = p_{0z}/\sqrt{M_N^2 + p_{0z}^2}$ ,  $\gamma = 1/\sqrt{1-v^2}$ ,  $p_{0z}$  is the initial nucleon momentum in the c.m. system of two nuclei, and  $M_N$  is the nucleon mass. We name  $t_c$  as the fireball formation time. The values of  $t_c$  are very close to the time moments which correspond to the first maximum of the reaction frequency (thick solid lines in Fig. 4). Slight difference of  $t_c$  and the time point of the real maximum can be explained by some decrease of a nucleon velocity which is due to inelastic and elastic reactions (stopping) of nucleons. Inelastic and elastic hadron collisions dominate at the first stage,  $t < t_c$ , of nucleus-nucleus collision. At later times, the elastic, decay and fusion reactions become more significant. We note that decay processes become the dominant ones after  $t \sim 10$  fm/c. After the full overlap of the nuclei, the created system begins to expand in space, which results in the decrease of the reaction rates. At the same time, the number of secondary particles still increases, resulting in an increase of the total reaction integral rate. Hence, the rate of expansion of the system and its ratio to the creation rate of secondary particles will determine the result of the competition of these two tendencies.

The contribution of the secondary particles becomes more significant at the later stage of collision, especially at SPS energies. The number of secondary particles (mainly  $\pi$  mesons) is approximately  $\langle n_\pi \rangle \simeq 0.6 \dots 1.6$  per nucleon for AGS conditions [10] and  $\langle n_\pi \rangle \simeq 2 \dots 6$  for SPS conditions [11, 12]. Such an increase of the number of secondary particles with the collision energy leads to the sufficient change of the reaction frequency's time dependence. Namely, for AGS conditions after  $t_c$ , the frequency of all reactions goes down. For SPS conditions, one can see the second local maximum of the reaction frequency (see thick solid line in Fig. 4) which is a consequence of a large number of reactions with secondary particles. At later times, the reaction frequency goes down, which results in fireball division into two parts at the time moment  $t = t_{fd}$  and the further breakup. The fireball division time is defined as the minimum value of time on the space-like hypersurface, which bounds the region of the cold fireball (blue area) from above, i.e.,  $t_{fd} \equiv t(z)|_{z=0}$  (see Fig. 3). We note that

the time moment  $t_{fd}$  depends very weakly on the collision energy.

It is seen that after the time moment  $t_{fd}$ , the rates of elastic and inelastic reactions vanish. That is, since this moment, the system behavior is determined mainly by the individual properties of particles (basically resonances). That is why, in spite of the sufficient difference of collision energies of the experiments under consideration, the times  $t_{fd}$  are approximately the same (see Fig. 3). If we compare the longitudinal sizes of the fireballs  $2R_z$  at the time moment  $t = t_{fd}$ , we see that they are approximately the same and equal to  $R_z = v t_{fd}$  [ $v$  is defined in Eq. (7), see Fig. 3]. This fact can explain the weak dependence of the pion interferometric radius  $R_L$  on the beam energy,  $R_L \propto R_z$  [13]. It can be claimed that the fireball achieves its maximum longitudinal size at the time moment  $t = t_{fd}$ , when it is divided into two parts.

#### 4. DISCUSSION AND CONCLUSIONS

Different parameters may be used to analyze the fireball evolution. In Fig. 5 we show four representations of the fireball which were obtained with making use of the microscopic transport model UrQMD for SPS conditions (Pb-Pb,  $E_{kin} = 158A$  GeV). First column shows the particle positions of all hadrons at different time moments. In second column the fireball is represented with the help of the energy density. Reaction density at different time moments is shown in third column. One can see that starting from the times  $t \approx 25$  fm/c the fireball representation given by the reaction density sufficiently differs from the one given by the energy density. For example, it is seen that there are no reactions in the central part of the system at large enough times while energy density there is still high. This situation may occur, e.g., when particles move in the same direction with some collective velocity without collisions. In the fourth column the coordinates of the last reactions of all particles are shown. It is, in fact, a depiction of a continuous kinetic freeze-out. One can see that the fireball representations in the third and fourth columns are qualitatively similar and they differ from one another just in the early stage of a fireball evolution.

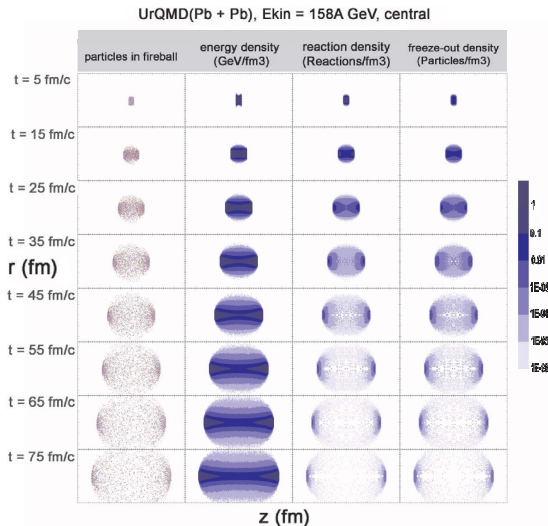


**Fig. 5.** Different fireball representations for SPS conditions,  $E_{\text{kin}} = 158A$  GeV

Our approach allows to investigate the spatial and temporal structures of the hadron system created in relativistic nucleus-nucleus collisions in terms of all hadronic reactions which occur in the system. In other words, the fireball is identified as the system of interacting hadrons. The proposed algorithm gives possibility to separate with a given accuracy the space-time region where the most intensive hadron reactions take place, i.e. we give the method to see a reaction zone in 3D representation (see Figs. 1, 2) and in different projections.

In the present microscopic study, we separate a fireball into the following regions, which characterize its evolution (see Fig. 3): (1) a hot fireball region, where 99% of all inelastic hadronic reactions have occurred (medium-grey or red), (2) a cold fireball region (dark-grey or blue), which together with the hot fireball contains 99% of all hadronic reactions  $N_{\text{tot}}$ , and (3) a fireball halo, where 0.9% of all hadronic reactions, i.e.,  $0.009N_{\text{tot}}$ , have occurred (light-grey or cyan). Two last regions together are a space-time region containing the hadron-resonance gas, and the reactions in this region are mainly presented by decays of resonances.

The study of hadron reaction zones allows one to analyze the freeze-out process in relativistic nucleus-nucleus collisions. An important question that can be clarified by the study of the reaction zones is how the space-time boundary of a fireball is related to the so-called sharp freeze-out hypersurface. In the literature, the sharp freeze-out hypersurface is usually defined with the help of some parameter  $P(t, \mathbf{r})$  which takes the critical value  $P_c$  on the hypersurface. That is, the equation of the hypersurface has form  $P(t, \mathbf{r}) = P_c$ . As such a parameter, one may choose the energy density  $\epsilon(t, \mathbf{r})$  [2], temperature  $T(t, \mathbf{r})$  [3, 4], particle density  $n(t, \mathbf{r})$  [1], etc. And the “classical” definition of the sharp kinetic freeze-out assumes the Cooper-Frye picture [14]: a radiation of free particles or a freeze-out process takes place within a thin layer determined by the hyper-

surface. It means, the initial value problem for the radiation corresponds to a space-like piece of the hypersurface whereas the boundary conditions for the radiative system correspond to a time-like part of the hypersurface. On the other hand, if we determine the reaction zone as that one, which contains, for instance, 99% of all reactions, then we can claim that the sharp kinetic freeze-out hypersurface should be definitely inside the boundary between the zone of a cold fireball and the fireball halo (see Fig. 3).

Assuming that the chemical freeze-out occurs when the inelastic reactions are completed [15], we can also claim that the chemical freeze-out hypersurface should be inside the reaction zone, which contains 99% of all inelastic reactions (red zone).

In the coordinates  $(t, z)$ , the curve, which is the upper space-like boundary of the “blue” zone, is a hyperbola of the form  $t(z) = A\sqrt{\tau_0^2 + z^2}$ , where  $A = 0.65$ ,  $\tau_0 = 46$  fm/c for the AGS energy ( $E_{\text{kin}} = 10.8A$  GeV) and  $A = 0.95$ ,  $\tau_0 = 38$  fm/c for the SPS energy ( $E_{\text{kin}} = 158A$  GeV). It is clear that the *fireball division time* is related to the parameters of the hyperbola in the following way  $t_{\text{fd}} = A\tau_0$  and we obtain  $t_{\text{fd}} \approx 30$  fm/c for AGS ( $E_{\text{kin}} = 10.8A$  GeV) and  $t_{\text{fd}} \approx 36$  fm/c for SPS ( $E_{\text{kin}} = 158A$  GeV). The lower time-like hypersurface bounding a cold fireball has the form of a straight line  $t(z) = t_0 + (z/v)$ , where  $t_0$  is close to zero, and  $v = 0.8$  for AGS energies and  $v = 0.98$  for SPS energies. For AGS energies, the time-like boundaries of the reaction zones differ significantly from one another and the light cone (Fig. 3). However, at higher SPS energies, for example, at  $E_{\text{kin}} = 158A$  GeV, the time-like hypersurfaces bounding all three zones of a fireball practically coincide with one another and are close to the light cone (Fig. 3). Thus, we can predict that this behavior will result in all time-like hypersurfaces merging on the energies available at the BNL Relativistic Heavy Ion Collider (RHIC) and coinciding with the light cone.

By studying the time dependence of the reaction frequency for different reaction types, we conclude that total reaction rate is dominated by elastic and inelastic hadron collisions at the early stage, whereas individual particles properties (basically resonances) determine system behavior at later stages. We also conclude that there are two specific time points in the evolution of a hadron fireball: the fireball formation time  $t_c$  defined as the time of the full overlap of two nuclei [Eq. (7)] and the fireball division time  $t_{\text{fd}}$ , which corresponds to the separation of the fireball into two individual parts and which depends weakly on the collision energy. At SPS energies there is also a second local maximum which is a consequence of a large number of reactions involving secondary particles.

## Acknowledgements

D. Anchishkin was supported by the program “Fundamental properties of physical systems under extreme conditions” (Division of the Physics and Astronomy of the NAS of Ukraine).

## References

1. D. Adamova et al. (CERES Collaboration). Universal Pion Freeze-out in Heavy-Ion Collisions // *Phys. Rev. Lett.* 2003, v. 90, 022301.
2. V.N. Russkikh and Y.B. Ivanov. Dynamical Freeze-out in 3-Fluid Hydrodynamics // *Phys. Rev.* 2007, v. C76, 054907.
3. H. von Gersdorff, L. McLerran, M. Kataja, and P.V. Ruuskanen. Studies of the hydrodynamic evolution of matter produced in fluctuations in p-p collisions and in ultrarelativistic nuclear collisions // *Phys. Rev.* 1986, v. D34, p. 794-810.
4. P. Huovinen. Chemical freeze-out temperature in hydrodynamical description of Au+Au collisions at  $\sqrt{s_{NN}} = 200$  GeV // *Eur. Phys. J.* 2008, v. A37, p. 121-128.
5. B. Tomasik and U.A. Wiedemann. The freeze-out mechanism and phase-space density in ultrarelativistic heavy-ion collisions // *Phys. Rev.* 2003, v. C68, 034905.
6. C.M. Hung and E. Shuryak. Equation of state, radial flow, and freeze-out in high energy heavy ion collisions // *Phys. Rev.* 1998, v. C57, p. 1891-1906.
7. D. Anchishkin, A. Muskeyev, and S. Yezhov. Relativistic nucleus-nucleus collisions: Zone of reactions and space-time structure of fireball // *Phys. Rev.* 2010, v. C81, 031902.
8. S.A. Bass et al. Microscopic Models for Ultra-relativistic Heavy Ion Collisions // *Prog. Part. Nucl. Phys.* 1998, v. 41, p. 255-369.
9. M. Bleicher et al. Relativistic Hadron-Hadron Collisions in the Ultra-Relativistic Quantum Molecular Dynamics Model // *J. Phys.* 1999, v. G25, p. 1859-1896.
10. J.L. Klay et al. (E895 Collaboration). Charged pion production in 2A to 8A GeV central Au+Au Collisions // *Phys. Rev.* 2003, v. C68, 054905.
11. C. Alt et al. (NA49 Collaboration). Pion and kaon production in central Pb+Pb collisions at 20A and 30A GeV: Evidence for the onset of deconfinement // *Phys. Rev.* 2008, v. C77, 024903.
12. S.V. Afanasiev et al. (NA49 Collaboration). Energy dependence of pion and kaon production in central Pb+Pb collisions // *Phys. Rev.* 2002, v. C66, 054902.
13. J. Chen (for STAR Collaboration). Particle Production in Au+Au Collisions at  $\sqrt{s_{NN}} = 9.2$  GeV // *CPOD2009 Proceedings*, Trieste, Italy, 2009.
14. F. Cooper and G. Frye. Single-particle distribution in the hydrodynamic and statistical thermodynamic models of multiparticle production // *Phys. Rev.* 1974, v. D10, p. 186-189.
15. U. Heinz. The Little Bang: searching for quark-gluon matter in relativistic heavy-ion collisions // *Nucl. Phys.* 2001, v. A685, p. 414-431.

## ЭВОЛЮЦИЯ АДРОННОЙ СИСТЕМЫ В РЕЛЯТИВИСТСКИХ СТОЛКНОВЕНИЯХ ТЯЖЕЛЫХ ИОНОВ

*Д.В. Анчишкин, А.О. Мускеев, В.Ю. Вовченко, С.Н. Ежов*

Эволюция адронной системы в релятивистских ядро-ядерных столкновениях изучена с помощью плотности реакций. Трехмерная зона реакций, а также ее проекции рассчитаны для энергий AGS и SPS с помощью микроскопической транспортной модели UrQMD. На основе проведенных вычислений частоты адронных реакций получены характерные точки во временной эволюции фаербола. Гиперповерхности, являющиеся границами зон реакций, соотносятся с процессами кинетического и химического фризаутов. Представление фаербола с помощью плотности реакций сравнивается с другими возможными представлениями.

## ЕВОЛЮЦІЯ АДРОННОЇ СИСТЕМИ В РЕЛЯТИВІСТСЬКИХ ЗІТКНЕННЯХ ВАЖКИХ ІОНІВ

*Д.В. Анчишкін, А.О. Мускеев, В.Ю. Вовченко, С.М. Єжов*

Еволюцію адронної системи в релятивістських ядро-ядерних зіткненнях досліджено за допомогою густини реакцій. Тривимірну зону реакцій, а також її проекції розраховано для енергій AGS та SPS за допомогою мікроскопічної транспортної моделі UrQMD. На основі проведених розрахунків частоти адронних реакцій отримані характерні точки у часовій еволюції фаербола. Гіперповерхні, що є границями зон реакцій, співвідносяться із процесами кінетичного та хімічного фрізаутів. Представлення фаербола за допомогою густини реакцій порівнюється із іншими можливими представленнями.